

Mechanobiology in the development, maintenance, and degeneration of articular cartilage

Gary S. Beaupré, PhD; Sheila S. Stevens, PhD; Dennis R. Carter, PhD

Rehabilitation Research and Development Center, VA Palo Alto Health Care System, Palo Alto, CA 94304;
Biomechanical Engineering Division, Mechanical Engineering Department, Stanford University, Stanford, CA
94305; Kyphon Inc., 3110 Coronado Drive, Santa Clara, CA 95054

Abstract—During skeletal development, the establishment of a layer of cartilage at the ends of long bones is intimately linked to the process of endochondral ossification. Previous *in vivo* studies and computer models suggest that mechanobiological factors can play a key role in modulating cartilage growth and ossification. Specifically, intermittent hydrostatic pressure is thought to maintain cartilage, and shear stresses encourage cartilage destruction and ossification. In the present investigation we examined the combined effects of hydrostatic pressure and shear stress—in the form of an osteogenic index—on the development of a layer of articular cartilage, using an idealized finite element computer model. The results of our analyses provide further support for the view that mechanobiological factors play a key role in regulating the distribution of cartilage thickness and in maintaining a stable cartilage layer at maturity. The model predicts that joints that experience higher contact pressures will have thicker cartilage layers. These predictions are consistent with observations of cartilage thickness in both humans and animals. Variations in articular mechanical load are

predicted to modulate cartilage thickness. These results are consistent with the view that the mechanobiological factors responsible for the development of diarthrodial joints eventually lead to cartilage degeneration and osteoarthritis (OA) with aging.

Key words: *cartilage thinning, computer modeling, endochondral ossification, hydrostatic stress, mechanobiology, osteoarthritis (OA), shear stress.*

INTRODUCTION

Primary or idiopathic osteoarthritis (OA) is a progressive disease characterized by the destruction of articular cartilage. The most common type of arthritis, OA, resulting in joint pain, stiffness, and limitations in activity, affects one out of every eight Americans aged 25 and older (1). Prevalence increases with age, resulting in one out of every two Americans aged 65 and older having some form of arthritis (2). Due to the aging of our society, this prevalence is projected to increase in the future (1). Arthritis is the leading chronic medical condition and the leading cause of disability for individuals over the age of 65 (2). The total cost of arthritis in the United States in 1992 was \$65 billion (3), representing more than 40 percent of the cost of all musculoskeletal impairments combined (2).

This material is based on work supported by the Department of Veterans Affairs, Washington, DC 20420.

Dr. Beaupré is the Associate Director of the VA Palo Alto Rehabilitation R&D Center and a Consulting Professor in the Biomechanical Engineering Division at Stanford University. Dr. Stevens is an R&D Engineer with Kyphon Inc. Dr. Carter is the Director of the VA Palo Alto Rehabilitation R&D Center and a Professor in the Biomechanical Engineering Division at Stanford University.

Address all correspondence and requests for reprints to: Gary S. Beaupré, PhD, Rehabilitation R&D Center (153), VA Palo Alto Health Care System, 3801 Miranda Avenue, Palo Alto, CA 94304; email: beaupre@bones.stanford.edu.

Osteoarthritis can be considered as the final stage in the process of endochondral ossification during ontogeny (4–6). During skeletal development, cartilage templates of the future long bones change in size and shape and are gradually replaced by bone through the process of endochondral ossification. The morphogenesis of the human femur is representative of this developmental process in mammalian long bones. About 7 weeks after fertilization and just prior to the first appearance of bone, a distribution of cartilage maturity exists within the cartilage anlage, with the most mature cartilage located at the midshaft and the least mature cartilage located near the bone ends (7). Bone first appears as a perichondral bony collar at the femoral midshaft, surrounding the most mature cartilage. Within the bony collar, vascular invasion of the hypertrophic chondrocytes triggers a sequence of events including calcification of the cartilage matrix, resorption of the calcified matrix, transient bone deposition on the cartilage erosion bays, and bone resorption, leading to the development of a marrow-filled cavity surrounded by the expanding collar of cortical bone.

The advance of the primary ossification front toward the epiphysis at each end of the femur proceeds at the same rate as the longitudinal advance of the perichondral bone collar. In long bones such as the femur, humerus, tibia, radius, and ulna, one or more secondary ossification centers form postnatally in each chondroepiphysis as the primary growth front approaches the chondroepiphysis. The region of cartilage between the primary and secondary ossification fronts delineates the growth plate and is responsible for the majority of longitudinal growth throughout skeletal development. The cartilage surrounding the secondary ossification center has a radial distribution of maturity, with the most mature cartilage adjacent to the ossific nucleus and the least mature cartilage near the periphery of the epiphysis (8). Growth of the cartilage and spherical ossification front surrounding the secondary epiphyseal bone center leads to expansion of the epiphysis. Advancement of the spherical ossification surface toward the bone end progressively defines a layer of articular cartilage at the joint surface. Thickness of the articular cartilage in the mature joint is determined by the distance from the joint surface at which endochondral ossification stabilizes.

Despite the relative stabilization of articular cartilage thickness at skeletal maturity, endochondral ossification within the cartilage layer does not entirely cease. Several studies have shown that the interface between articular cartilage and subchondral bone remains active

throughout life and is responsible for the gradual changes in joint shape that occur with aging (9,10). In an experimental study in mature rabbits, Haynes (11) has shown that the tidemark separating unmineralized cartilage from calcified cartilage continually advances toward the articular surface and that the advancement is greatest in non-weightbearing areas. Lane and Bullough (10) have shown that in human femoral and humeral heads, the number of tidemarks increases markedly after the age of 60, indicating a reactivation of endochondral ossification with aging. The exact cause of this increased rate of endochondral ossification remains unknown.

Epigenetic Regulation of Endochondral Ossification

Clinical observations (12,13), *in vivo* studies (13), and computer modeling (4,14–18) indicate that mechanical loading is a potent epigenetic regulator of endochondral ossification. Mechanical regulation may act in part through changes in biosynthesis and/or catabolism of angiogenic and antiangiogenic factors.

The observation that mechanical stimuli can modulate cartilage growth and ossification is not new. In 1862, Hueter (19) and Volkmann (20) proposed that cartilage growth is regulated by compressive stress. In spite of its somewhat simplistic uniaxial representation of stress, the Hueter-Volkmann law remains as one of the guiding tenets in the treatment of orthopedic growth abnormalities today. Simon (21) and Frost (22) have introduced alternative formulations of chondral mechanoregulation, both of which are based on uniaxial stress approaches.

Carter and colleagues (14,17,23,24) developed an approach for the regulation of cartilage growth and ossification based on the concept that intermittent hydrostatic pressure will maintain cartilage and that shear stresses will encourage cartilage destruction and ossification. These investigators introduced a scalar parameter called the osteogenic index to integrate the competing effects of hydrostatic and shear stresses. When combined with a stress analysis, the osteogenic index can be used to predict which regions of a cartilaginous skeletal element are likely to ossify first and which regions are likely to remain cartilaginous. Using the osteogenic index formulation, Carter and Wong (14) performed a computer simulation of the chondroepiphysis at the end of an idealized long bone, focusing on the appearance and development of the secondary center of ossification. The predicted appearance, location, and shape of the secondary ossification center in the developing chondroepiphyses in their model were consistent with clinical observations (**Figure 1**).

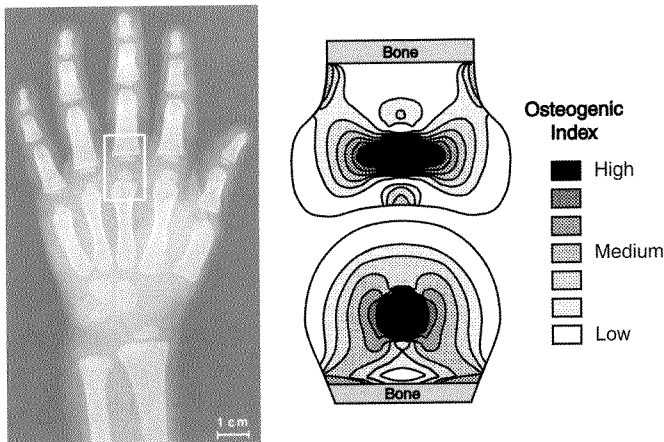


Figure 1.

Left: Radiograph of the hand of a 32-month-old child, showing a round secondary ossification center in the distal metacarpal and a flattened ossification center in the proximal end of the proximal phalanx. (From Radiographic Atlas of Skeletal Development of The Hand and Wrist, Second Edition, by William Walter Greulich and S. Idell Pyle. Used with permission of the publishers, Stanford University Press. Copyright 1950, 1959 by the Board of Trustees of the Leland Stanford Junior University; reference 25). Right: Distribution of osteogenic index in an idealized model of a diarthrodial joint. The predicted appearance, location, and shape of the secondary ossification centers in the developing chondroepiphyses are consistent with clinical observations. (Adapted with permission from 5.)

In a reexamination of the chondroepiphysis model of Carter and Wong (14), Stevens et al. (15) introduced a modification to the definition of the original osteogenic index (23), with the modified osteogenic index, $OI_{\max\min}$, defined as:

$$OI_{\max\min} = \text{Max}_{i=1,n} \bar{\sigma}_{si} + k \text{Min}_{i=1,n} \bar{\sigma}_{hi} \quad [1]$$

where $\text{Max}_{i=1,n} \bar{\sigma}_{si}$ is the maximum value of shear stress and $\text{Min}_{i=1,n} \bar{\sigma}_{hi}$ is the minimum (most compressive) value of hydrostatic stress for a series of discrete load cases, $i=1$ to n . According to our theory, the more positive the value of the osteogenic index, the higher the stimulus for ossification; the more negative the value, the greater the stimulus for cartilage maintenance. We should note that the octahedral shear stress is a positive quantity, while hydrostatic stress is negative for compression and positive for tension. Thus, shear stress and tensile hydrostatic stress increase the value of the osteogenic index but compressive hydrostatic stress decreases its value. One advantage of the $OI_{\max\min}$ formulation is that its value does not change, for example, simply by doubling the number of loading cycles for each load case, whereas the original osteogenic index (17) would double in value for this scenario. In Equation 1, the parameter k is an empirical con-

stant that weights the relative importance of hydrostatic and shear stress. Previous studies have shown that the best correspondence between model predictions and clinical observations is obtained by choosing k in the range of 0.35 to 1.0 (14–18).

In our previous studies of the developing chondroepiphysis, the region of highest osteogenic index corresponds to the location of the secondary ossification center. As the secondary ossification center expands radially toward the joint surface, we hypothesize that endochondral ossification stabilizes in response to the tissue's mechanical stress state and that a layer of articular cartilage is progressively defined. In the present study we will use the osteogenic index to examine this process more closely and to suggest new insights into the role of mechanobiology in the development, maintenance, and degeneration of articular cartilage.

METHODS

To examine the role of mechanobiology in the development of articular cartilage, we created a series of finite element models of a simplified joint (15). A typical model consisted of three material layers corresponding to articular cartilage, subchondral bone, and a cancellous bone bed, with a combined thickness of 20 mm (Figure 2). The calcified cartilage at the base of the articular cartilage was not explicitly modeled. The thick-

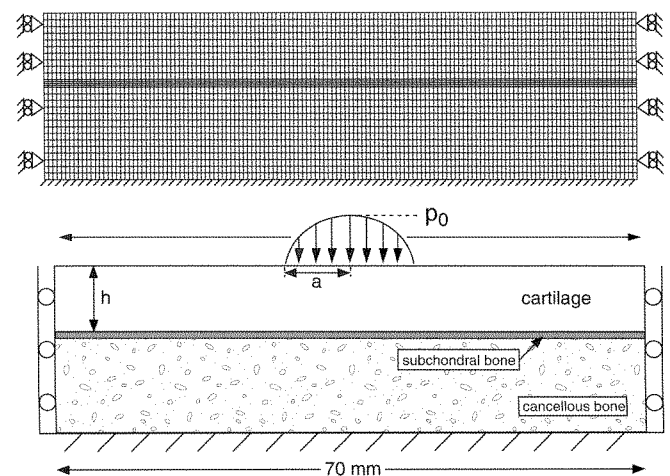


Figure 2.

Finite element model of a simplified joint. The model consists of three material layers corresponding to articular cartilage, subchondral bone, and a cancellous bone bed, with a combined thickness of 20 mm. (Adapted with permission from 26.)

ness, h , of the cartilage layer was varied from 0.5 to 20 mm in order to examine the changes that occur as the cartilage layer decreases in thickness during development. The model that had a 20-mm-thick layer of cartilage had no subchondral bone or cancellous bone. All other models had a 1-mm-thick layer of subchondral bone and a layer of cancellous bone, the thickness of which made up the balance of the 20-mm total thickness. The linear elastic material properties for the three layers are given in **Table 1**.

Table 1.
Elastic properties.

Material	Elastic Modulus (MPa)	Poisson's Ratio
Cartilage	6	0.49
Subchondral bone	2,000	0.30
Cancellous Bone	600	0.30

The applied loading consisted of a Hertzian-shaped pressure distribution (27) with a peak magnitude, p_0 , which varied between 1.0 and 10.0 MPa, and a contact radius, a , equal to 5.0, 10.0, or 20.0 mm. The pressure loading was swept across the entire extent of the cartilage surface to simulate cyclic joint motion, such as the distal femoral condyle sweeping back and forth across the tibial condyle.

For each location within the cartilage layer, we calculated the minimum hydrostatic stress, maximum octahedral shear stress, and the osteogenic index, normalized in each case by the peak value of the applied pressure loading. The value of the weighting parameter, k , was chosen to be 0.35.

Final cartilage thickness was predicted as a function of peak applied pressure and contact radius. Final cartilage thickness was defined as that value of thickness for which the maximum value of the ossification stimulus was located at the cartilage/subchondral bone interface and the magnitude of the osteogenic index was below a critical value, assumed to be -500 KPa.

RESULTS

For the thickest cartilage layer ($h/a=2.0$), the hydrostatic pressure is greatest (most negative) at the articulating surface (**Figure 3**, bottom). In all cases, the pressure varies nonlinearly through the layer thickness. As the car-

tilage layer becomes thinner, the hydrostatic pressure through the layer becomes more uniform (**Figure 3**, top) and closer in magnitude to the value of the peak applied pressure. For the thinnest cartilage layer ($h/a=0.2$), the hydrostatic pressure varies by less than 5 percent from the top to the bottom of the cartilage layer and is similar in magnitude to the peak applied pressure.

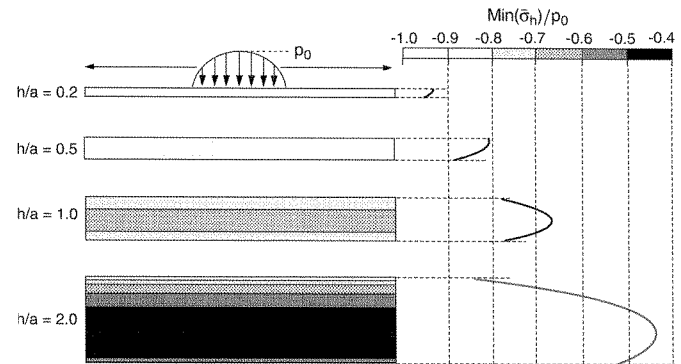


Figure 3.

The predicted distribution of hydrostatic stress is shown for each of four models having progressively thinner cartilage layers. For the thinnest cartilage layer ($h/a=0.2$), the distribution of hydrostatic pressure through the layer becomes more uniform and the magnitude approaches the value of the peak applied pressure. (Adapted with permission from 26.)

For the thickest cartilage layer ($h/a=2.0$), the octahedral shear stress has a maximum value located approximately 1/3 of the distance down from the surface (**Figure 4**, bottom). This finding is consistent with the classic Hertz solution describing contact between a spherical indenter

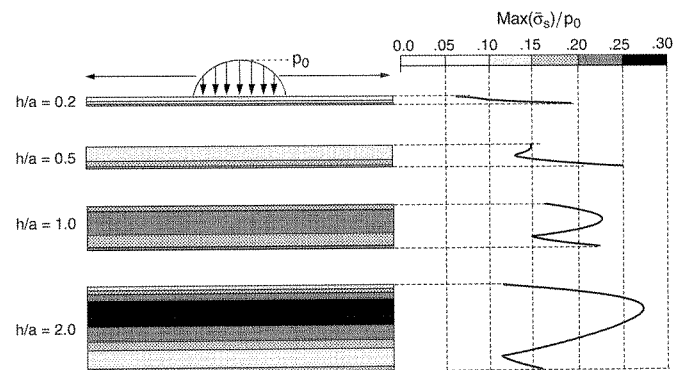


Figure 4.

The predicted distribution of octahedral shear stress is shown for each of four models having progressively thinner cartilage layers. For the thinnest cartilage layer ($h/a=0.2$), the location of maximum shear stress shifts to the cartilage/subchondral bone interface at the base of the cartilage layer. (Adapted with permission from 26.)

and an elastic substrate (27). For the Hertz problem, the maximum shear stress occurs at a subsurface location within the substrate. As the cartilage layer becomes thinner ($h/a=0.2$), the solution less resembles the Hertz situation, and the location of maximum shear stress shifts to the cartilage/subchondral bone interface at the base of the cartilage layer (Figure 4, top).

The distribution of osteogenic index for the different cartilage thicknesses is shown in Figure 5. For the thickest cartilage layer ($h/a=2.0$), the osteogenic index has its most positive value (ossification promoting) located approximately 40 percent down from the surface and its most negative value (cartilage preserving) at the articulating surface (Figure 5, bottom). For the thinnest cartilage layer ($h/a=0.2$), the osteogenic index distribution indicates that the articulating surface is exposed to the most cartilage-preserving stimuli and the cartilage/subchondral bone interface is exposed to the most ossification-promoting stimuli (Figure 5, top). The predicted distribution of osteogenic index for the thickest cartilage layer model is nearly identical to that predicted for the developing chondroepiphysis (Figure 6).

Figure 7 is a graph of final cartilage thickness as a function of the peak applied pressure magnitude and contact radius. For a given contact radius, cartilage thickness is predicted to increase with increasing applied joint pressure. For a given peak applied pressure, cartilage thickness is predicted to increase with increasing contact radius.

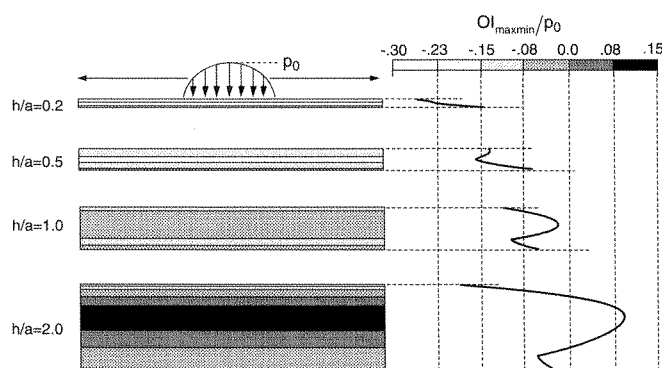


Figure 5.

The predicted distribution of osteogenic index is shown for each of four models having progressively thinner cartilage layers. For the thinnest cartilage layer ($h/a=0.2$), the distribution of osteogenic index indicates that the articulating surface is exposed to the most cartilage-preserving stimuli, while the cartilage/subchondral bone interface is exposed to the most ossification-promoting stimuli. (Adapted with permission from 26.)

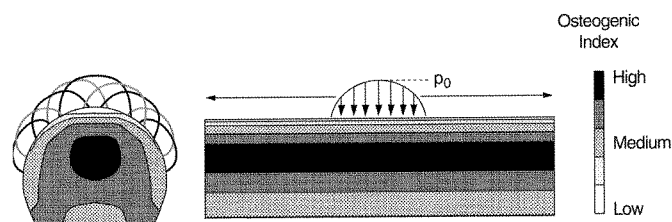


Figure 6.

The predicted distribution of osteogenic index within the developing chondroepiphysis in comparison with the predicted distribution of osteogenic index for the thickest cartilage layer model. These two models show nearly identical distributions of the osteogenic index. (Adapted with permission from 26.)

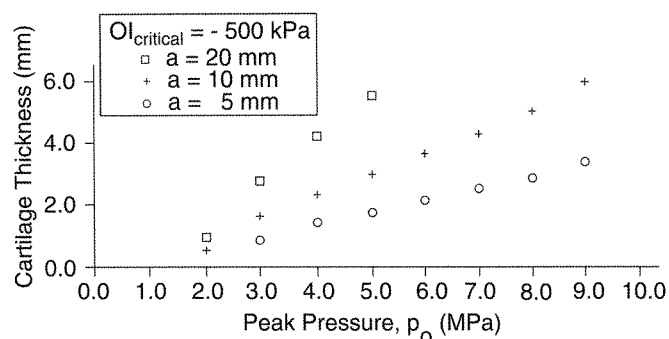


Figure 7.

The predicted cartilage thickness is plotted as a function of the magnitude of the peak cyclic joint pressure (p_0) for three different values of the joint contact radius (a). Increased cartilage thickness is predicted with increased joint pressures. (Adapted with permission from 26.)

DISCUSSION

In the course of endochondral growth and ossification, cartilage undergoes the normal sequence of proliferation, maturation, hypertrophy, calcification, and ossification. Biochemical factors play important roles in this sequence of events. The avascularity of normal adult hyaline cartilage provides one such example. Maintenance of an avascular environment surrounding resting and proliferating chondrocytes is due in part to synthesis, by the chondrocytes, of multiple antiangiogenic factors (28). Cartilage-derived inhibitor (29), chondromodulin-I (30), and troponin I (31) have been isolated from normal cartilage and shown to inhibit neovascularization, typically by limiting endothelial cell development. The presence of these factors may be critical for preventing angiogenesis, thereby slowing endochondral ossification and maintaining healthy cartilage. The treatment of OA via the administration of antiangiogenic compounds was suggested in

anticipation of the pharmacological use of such compounds (32).

Although resting and proliferating chondrocytes produce antiangiogenic factors, hypertrophic chondrocytes and degenerating cartilage produce factors known to promote angiogenesis and neovascularization (33), prerequisites for ossification. Angiogenesis is achieved by the growth of endothelial sprouts that migrate into new tissue regions. The magnitude and direction of the new vascular ingrowth is regulated by local concentrations of angiogenic factors. One angiogenic factor associated with endochondral ossification is transferrin (34), a molecule released by hypertrophic chondrocytes. Other substances, such as the breakdown products of the cartilage extracellular matrix constituent, hyaluronic acid, are also known to be angiogenic (35). Although the angiogenic properties of cartilage proteoglycans such as aggrecan are unknown, there is evidence that proteoglycan degradation is permissive for cartilage calcification (36,37).

The results of our computer models suggest that the mechanobiological stimulus for endochondral ossification decreases as the articular cartilage thins, and when the stimulus falls below a critical level, endochondral ossification ceases and the distribution of mature cartilage thickness is established. For higher joint contact pressures, our models predict that cartilage thickness will increase. This is consistent with observations in human joints that cartilage thickness tends to be greatest in joints that experience high forces and high joint contact pressures. During life, changes in customary use of joints will induce concomitant changes in cartilage thickness. For example, increases in physical activity in young beagle dogs have been shown to increase both the thickness and proteoglycan content of articular cartilage (38). Reductions in physical activity from immobilization lead to cartilage thinning in rabbits (39). Increased cartilage thickness with increased joint pressure is also consistent with correlations between animal size and cartilage thickness (40) showing that larger animals with higher joint pressures (41) have thicker cartilage.

Changes in daily physical activity with aging typically lead to alterations and reductions in joint loading. These changes, in turn, can alter the mechanobiology at the cartilage/subchondral bone interface, reactivating endochondral ossification, resulting in cartilage thinning and degeneration. Although it is clear that the resulting changes in chondrocyte synthesis of matrix proteins may occur either as a direct result of aging or as a result of changes in loading history, the cellular mechanisms by

which this process is orchestrated remain the topic of intense research.

CONCLUSION

The results of this study suggest that primary or idiopathic OA is the final stage of skeletal ontogeny. The regulation of endochondral ossification by mechanical stimuli results in the gradual replacement of cartilage by bone throughout life. Although this process is slowed dramatically at the articular surfaces throughout most of adulthood, the gradual destruction of cartilage and its replacement by bone accelerates with advancing age, particularly after the age of 60. The mechanobiology that is responsible for the efficient design of diarthrodial joints during development eventually leads to OA with aging. In the future, the development of new pharmacological agents used in combination with specific exercise regimens may slow or stop the reactivation of the endochondral ossification process and preserve healthy cartilage throughout life.

REFERENCES

1. Lawrence RC, Helmick CG, Arnett FC, Deyo RA, Felson DT, Giannini EH, et al. Estimates of the prevalence of arthritis and selected musculoskeletal disorders in the United States. *Arthritis Rheum* 1998;41(5):778-99.
2. Praemer A, Furner S, Rice DP. *Musculoskeletal conditions in the United States*. Park Ridge: American Academy of Orthopaedic Surgeons; 1992.
3. Callahan LF. The burden of rheumatoid arthritis: facts and figures. *J Rheumatol Suppl* 1998;53:8-12.
4. Carter DR, Orr TE, Fyhrie DP, Schurman DJ. Influences of mechanical stress on prenatal and postnatal skeletal development. *Clin Orthop* 1987;219:237-50.
5. Carter DR, Wong M. Mechanical stresses in joint morphogenesis and maintenance. In: Mow VC, Ratcliffe A, Woo SLY, editors. *Biomechanics of diarthrodial joints*, vol II. New York: Springer-Verlag; 1990. p. 155-74.
6. Carter DR, Beaupré GS. *Skeletal function and form*. In press, New York: Cambridge University Press.
7. Streeter GL. Developmental horizons in human embryos. *Contrib Embryol Carnegie Inst* 1949;34:165-96.
8. Serafini-Fracassini A, Smith JW. *The structure and biochemistry of cartilage*. Edinburgh & London: Churchill Livingstone; 1974.
9. Green WT, Martin GN, Eanes ED, Sokoloff L. Microradiographic study of the calcified layer of articular cartilage. *Arch Pathol* 1970;90(2):151-8.
10. Lane LB, Bullough PG. Age-related changes in the thickness of the calcified zone and the number of tidemarks in adult human articular cartilage. *J Bone Jt Surg* 1980;62-B(3):372-5.

11. Haynes DW. The mineralization front of articular cartilage. *Metab Bone Dis Rel Res* 1980;2:55–9.
12. Gardner E. Prenatal development of the human hip joint, femur, and hip bone. In: *AAOS Instructional Course Lectures*. St. Louis: C.V. Mosby; 1972. p. 138–54.
13. Trueta J. The normal vascular anatomy of the human femoral head during growth. *J Bone Jt Surg* 1957;39-B:358–93.
14. Carter DR, Wong M. The role of mechanical loading histories in the development of diarthrodial joints. *J Orthop Res* 1988;6(6):804–16.
15. Stevens SS, Beaupré GS, Carter DR. Joint loading regulates the development of articular cartilage thickness. *Trans Orthop Res Soc* 1998;23:900.
16. Stevens SS, Beaupré GS, Carter DR. Computer model of endochondral growth and ossification in long bones: biological and mechanobiological influences. *J Orthop Res* 1999;17:646–53.
17. Wong M, Carter DR. Mechanical stress and morphogenetic endochondral ossification of the sternum. *J Bone Jt Surg* 1988;70-A(7):992–1000.
18. Wong M, Carter DR. A theoretical model of endochondral ossification and bone architectural construction in long bone ontogeny. *Anat Embryol (Berl)* 1990;181(6):523–32.
19. Hueter C. Anatomische Studien an den Extremitätengelenken Neugeborener und Erwachsener. *Virchows Arch* 1862;25:572–99.
20. Volkmann R. Chirurgische Erfahrungen ueber Knochenverbiegungen und Knochenwachstum. *Arch Pathol Anat* 1862;24:512–40.
21. Simon MR. The effect of dynamic loading on the growth of epiphyseal cartilage in the rat. *Acta Anat (Basel)* 1978;102(2):176–83.
22. Frost HM. A chondral modeling theory. *Calcif Tissue Int* 1979;28(3):181–200. 23. Carter DR. Mechanical loading history and skeletal biology. *J Biomech* 1987;20(11/12):1095–109.
24. Carter DR, Blenman PR, Beaupré GS. Correlations between mechanical stress history and tissue differentiation in initial fracture healing. *J Orthop Res* 1988;6(5):736–48.
25. Greulich WW, Pyle SI. Radiographic atlas of skeletal development of the hand and wrist. Stanford: Stanford University Press; 1959. p. 79.
26. Stevens SS. Mechanical regulation of articular cartilage development, maintenance and degeneration, in mechanical engineering. Stanford: Stanford University Press; 1997.
27. Timoshenko SP, Goodier JN. Theory of elasticity. New York: McGraw-Hill; 1970.
28. Kuettner KE, Pauli BU. Vascularity of cartilage. In: Hall BK, editor. *Structure, function and biochemistry*. (Cartilage; vol 1). New York: Academic Press; 1983. p. 218–312.
29. Moses MA, Sudhalter J, Langer R. Identification of an inhibitor of neovascularization from cartilage. *Science* 1990;248(4961):1408–10.
30. Shukunami C, Iyama K, Inoue H, Hiraki Y. Spatiotemporal pattern of the mouse chondromodulin-I gene expression and its regulatory role in vascular invasion into cartilage during endochondral bone formation. *Int J Dev Biol* 1999;43(1):39–49.
31. Moses MA, Wiederschain D, Wu I, Fernandez CA, Ghazizadeh V, Lane WS, et al. Troponin I is present in human cartilage and inhibits angiogenesis. *Proc Natl Acad Sci U S A* 1999;96(6):2645–50.
32. Simon WH, Lane JM, Beller P. Pathogenesis of degenerative joint disease produced by *in vivo* freezing of rabbit articular cartilage. *Clin Orthop* 1981;155:259–68.
33. Alini M, Marriott A, Chen T, Abe S, Poole AR. A novel angiogenic molecule produced at the time of chondrocyte hypertrophy during endochondral bone formation. *Dev Biol* 1996;176(1):124–32.
34. Carlevaro MF, Albini A, Ribatti D, Gentili C, Benelli R, Cermelli S, et al. Transferrin promotes endothelial cell migration and invasion: implication in cartilage neovascularization. *J Cell Biol* 1997;136(6):1375–84.
35. Liu D, Pearlman E, Diaconu E, Guo K, Mori H, Haqqi T, et al. Expression of hyaluronidase by tumor cells induces angiogenesis *in vivo*. *Proc Natl Acad Sci U S A* 1996;93(15):7832–7.
36. Eanes ED, Hailer AW. Effect of ultrafilterable fragments from chondroitinase and protease-treated aggrecan on calcium phosphate precipitation in liposomal suspensions. *Calcif Tissue Int* 1994;55(3):176–9.
37. Bulkwalter JA. Epiphyseal and physeal proteoglycans. In: Bulkwalter JA, Ehrlich MG, Sandell LJ, Trippel SB, editors. *Skeletal growth and development*. Rosemont, IL: American Academy of Orthopaedic Surgeons; 1998. p. 225–40.
38. Kirviranta I, Tammi M, Jurvelin J, Säämänen A-M, Helminen HJ. Moderate running exercise augments glycosaminoglycans and thickness of articular cartilage in the knee joint of young beagle dogs. *J Orthop Res* 1988;6(2):188–95.
39. Smith RL, Thomas KD, Schurman DJ, Carter DR, Wong M, van der Meulen MC. Rabbit knee immobilization: bone remodeling precedes cartilage degradation. *J Orthop Res* 1992;10(1):88–95.
40. Simon WH. Scale effects in animal joints: I. Articular cartilage thickness and compressive stress. *Arthritis Rheum* 1970;13(3):244–56.
41. Carter DR, Carter AJ, Beaupré GS. Allometry of cartilage thickness is influenced by developmental mechanobiology. *Proc Ann Mtg Soc Exp Bio*; 1999, Edinburgh. A9.13, p. 40.